EFFECTS ON SEED-BASED RESTING STATE FMRI OF ONE SEASON OF EXPOSURE TO MIDDLE SCHOOL AND HIGH SCHOOL FOOTBALL SUBCONCUSSIVE HEAD ACCELERATIONS

by

Xiaoyu Ji

A Thesis

Submitted to the Faculty of Purdue University

In Partial Fulfillment of the Requirements for the degree of

Master of Science in Electrical and Computer Engineering

Electrical and Computer Engineering

West Lafayette, Indiana

May 2021

THE PURDUE UNIVERSITY GRADUATE SCHOOL
STATEMENT OF COMMITTEE APPROVAL

Dr. Thomas M. Talavage, Chair

School of Electrical and Computer Engineering

Dr. Charles A. Bouman

School of Electrical and Computer Engineering

Dr. James S. Lehnert

School of Electrical and Computer Engineering

Approved by:

Dimitrios Peroulis

ACKNOWLEDGMENTS

This thesis work would not be possible without the guidance of Prof. Thomas Talavage, I would like to express my great gratitude for the expert advice and encouragement he gave me. Thanks to all the colleagues in EE30 lab for their great help.

TABLE OF CONTENTS

LIST OF TABLES 6

LIST OF FIGURES 7

ABBREVIATIONS 9

ABSTRACT 10

1 INTRODUCTION 11

2 BACKGROUND 13

2.1 Resting State fMRI and Functional Connectomes 13

2.2 Resting State Networks 14

2.3 Seed based Functional Connectivity Analysis 15

2.4 The Identifiability Matrix 16

2.5 Repetitive HAEs 17

3 METHODS 18

3.1 Participants 18

3.2 Data collection 18

3.3 Data processing pipeline 19

3.4 Data analysis 20

3.4.1 Consistency and identification analysis 20

3.4.2 Yeo resting state networks analysis 21

3.4.3 Seed based region of interests 21

3.4.4 ICC analysis 22
3.4.5 Seed-based identification analysis 24
3.4.6 PLA data analysis 24
4 RESULTS 26
5 DISCUSSION 38
5.1 Brief Summary 38
5.2 Yeo networks identification comparison 39
5.3 Age dependence in seed based ROI 40
5.4 HAE influence to ICC 40
5.5 Identification and consistency measurements for different age group 41
5.6 PLA related hypothesis 42
6 CONCLUSION 44
REFERENCES 45

LIST OF TABLES

4.1 Middle school and high school in-network identifiability matrix yeo1 to yeo4 . . 27

4.2 Middle school and high school in-network identifiability matrix yeo5 to yeo7 . . 28

4.3 Variation ratio of six Yeo networks. Variation ratio represents percentage of increase from middle school mean I_{diff} to high school mean I_{diff}. 29

4.4 Kruskal-Wallis test between I_{self} values in identifiability matrix of control group and that of other player groups in Figure 4.7 36

LIST OF FIGURES

3.1 Middle School seed based ROI count and the threshold of player count. If x is 5, then corresponding y value is the number of ROIs correlated with seed for 5 players at the same time. 23

4.1 Yeo identifiability matrices I_{diff} comparison between middle school and high school players 29

4.2 Yellow regions are DMN network and red regions are ROIs highly correlated with PCC for all players ($p<0.05$). Grey background is shen278 parcellations and there are 278 ROIs with different grey level. (a): there are 16 ROIs in red regions, 10 overlap with the DMN mask(yellow regions); (b): there are 14 ROIs in red regions, 7 overlap with DMN mask(yellow regions). There are 6 different ROIs between pre-season and post-season seed-based maps. 30

4.3 Yellow regions are DMN network and red regions are ROIs highly correlated with PCC for all players ($p<0.05$). Grey background is shen278 parcellations and there are 278 ROIs with different grey level. (a): there are 18 ROIs in red regions, 11 overlap with the DMN mask(yellow regions); (b): there are 18 ROIs in red regions, 11 overlap with DMN mask(yellow regions). There are 5 different ROIs between pre-season and post-season seed-based maps. . . . 31

4.4 ICC matrix for high school players(a) and controls(b). Both are reduced to range from -0.1 to 0.3 in order to see detail matrix pattern. Any pixel value larger than 0.3 is marked as yellow, and that smaller than -0.1 is blue here. . 32

4.5 Distribution of high school ICC upper triangular values 33

4.6 High school seed-based identifiability matrix (a) and I_{diff} (b). (a): this matrix is a similarity comparison of post-season scan with pre-season scan. The horizontal axis represent post-season scans and the vertical axis represent pre-season scans. Rows and columns labeled with p are players, with c are controls. In total 15 players and 9 controls. 34

4.7 Middle school seed-based identifiability matrix (a) and I_{diff} (b). In total 11 players and 2 controls 35

4.8 Boxplot distribution of I_{self} in Figure 4.5 and 4.6. The five groups here are controls of middle school and high school, middle school 7th grade players, middle school 8th grade players, high school 15-16 years old players and high school 17-18 years old players 36

4.9 Count of events exceeding the indicated acceleration threshold and I_{self} scatter plot: (a-f) are the distribution of the number of events whose PLA larger than 20g, 30g, 40g, 50g, 60g and 70g. Red dots represent 17-18 years old high school data, magenta dots represent 15-16 years old high school data, blue dots represent 8th grade middle school data and cyan dots represent 7th grade middle school data. Correlation values in the titles are calculated from all the data points in the figure 37

ABBREVIATIONS

HAEs	head acceleration events
rs-fMRI	resting state functional magnetic resonance imaging
DMN	default mode network
TBI	traumatic brain injury
CTE	chronic traumatic encephalopathy
ROIs	regions of interest
PCC	posterior cingulate cortex
BOLD	blood oxygen level dependent
RSNs	resting state networks
FSL	FMRIB Software Library
MPFC	medial prefrontal cortex
AG	angular gyrus
SCA	seed-based functional connectivity analysis
ICA	independent component analysis
ACC	anterior cingulate cortex
PCA	principal component analysis
PLA	peak linear acceleration
DICOM	Digital Imaging and Communications in Medicine
FOV	field-of-view
AFNI	Analysis of Functional NeuroImages
GM	Gray Matter
MBWSS	Marker based watershed scalper toolbox
FWHM	full-width-at-half-maximum
ICC	intraclass correlation coefficient

ABSTRACT

Young football players are hypothesized to experience damage to the brain and brain function from repeated subconcussive head acceleration events (HAEs) during practices and games. Such damage may cause delayed cognitive and mental problems. Resting state fMRI (rs-fMRI) is an effective non-invasive method to detect alterations in brain functional connectivity. Seed-based rsfMRI analysis using the central node of the default mode network (DMN) as the seed is a common approach to measuring intrinsic changes of the DMN, accepted as a key network in brain function. Seed-based rs-fMRI analysis of the DMN was used to explore how age, HAE intensity, and HAE counts influence brain connectivity in youth athletes (ages 12-18). Middle school and high school football players and peer controls were studied using rs-fMRI before and after one season of competition. An identifiability matrix was generated from the seed-based connectivity matrix, allowing measurement of similarity between pre-season and post-season functional connectivity. The consistency of seed-based brain functional connectivity we observed across the season of play for players has no statistically significant difference from controls. The identifiability matrix exhibited no relation to the number and magnitude of any subset of HAEs experienced which rejected our hypothesis. Another finding is that high school football players exhibited the largest percentage increase in identification from middle school football players in the somatomotor network over other resting-state networks.

1. INTRODUCTION

High intensity contact sports, like football, soccer, rugby et al., are typified by repetitive impacts. Concussion is a mild form of traumatic brain injury (TBI) that damages brain function. Some serious brain injuries due to concussions such as Chronic Traumatic Encephalopathy (CTE) [1] can last lifelong and even be life threatening if untreated. Unlike diagnosable concussions, asymptomatic sub-concussive impacts can be easily ignored, especially for young players. Over half of high school football players were reluctant to report injuries due to unawareness or other reasons [2], [3]. However, in 2013 Bailes JE et al. [4] demonstrated that sub-concussive head acceleration events (HAEs) which is usually unknown by players would also lead to neurodegenerative pathology along with CTE. The influence of sub-concussive HAEs has thus received more and more attention and stimulated widespread interests.

For adolescent football players, research has been conducted to analyze whether concussion impacts are related to age factor, but relations between impacts of sub-concussive HAEs and age factors have not been analyzed. Even the answer to whether age influences sports concussion is not clear yet. Empirical studies believe that young players need a longer recovery time after concussions than older players [5]–[7], but statistical analysis of recovery times are small [8]. Brain white matter analysis can also fail to prove younger players are more susceptible than older ones [9]. Therefore, the influence of age on brain damage from HAEs needs to be researched.

HAE intensity and counts is another factor we want to consider. Studies have shown that the amount of impacts is significantly related to ensuing neurophysiological behavior of players [10]. Also, the effect of repetitive exposure is cumulative, which means 10 low acceleration blows have a stronger influence than one high acceleration blow [11], [12]. Due to the cumulative property of HAEs, an assumption has been made that players who received large counts of HAEs would have stronger functional connectivity alteration across the season of competition.

To measure brain functional connectivity, resting state fMRI (rs-fMRI) is an effective non-invasive method. Seed-based functional connectivity analysis is one of the most commonly

used functional integration rs-fMRI analyses method, which observes intrinsic changes in specific brain networks or regions of interest (ROIs) [13]. Of all the resting state brain networks, default mode network (DMN) is probably the most rudimentary one [14]. In 2015, Zhu et al. [15] illustrated that long-term variation of DMN can be used as a biomarker to detect functional brain changes of contact sport players. Using the central node of the DMN which is the posterior cingulate cortex (PCC) as the seed region, neurophysiological changes of high school players can be observed [16]. The identifiability matrix is also an effective measurement of functional connectivity alteration [17].

In this study, we analyzed functional connectivity alterations in male football players and peer controls in both middle school and high school across one season of play. Age and HAE counts of different intensity subsets were hypothesized to affect the alteration. Seed based rs-fMRI functional connectivity analysis and identifiability measurements were used to do age group and HAE intensity group comparison.

2. BACKGROUND

2.1 Resting State fMRI and Functional Connectomes

Functional MRI is a technique to capture brain regions which are activated by specific tasks or are low frequency fluctuation. The key principle of functional MRI is blood oxygen level dependent (BOLD) imaging, which is an imaging approach to detect changes in oxygen level and carbon dioxide level [13], [18]. Because brain neurons are not able to keep energy internally, all the strength of stimulation come from capillaries nearby. The process of capillaries providing energy to neurons is called haemodynamic response, which always appears along with oxyhemoglobin and deoxyhemoglobin. These processes can be successfully detected by BOLD imaging.

Functional MRI can be divided into two categories: rs-fMRI and task-based fMRI. Most of fMRI studies were task-based where participants are required to perform specific tasks (cognitive, language, or motor tasks) while scanning. This method helps analyze specific activated brain network corresponding to a certain experimental task, but actual detail variation in task implementation is difficult to evaluate, so operating error would be difficult to omit if task is not well designed. Some special instructions of tasks are even difficult for patients with neurologic or psychiatric problems to follow.

Compared to task-based method, rs-fMRI would be easier to realize. Participants need to stay awake and relax without doing any required task while scanning, so only asleep subjects need to be excluded. Besides, rs-fMRI takes shorter time for scanning which is a great benefit for participants with neural diseases such as attention deficit hyperactivity disorder. It is also convenient for researchers or clinicians because information can be collected within one fast scan. Biswal et al.in 1995 first figured out that low frequency oscillation (0.01-0.1Hz) reveals brain functional connectivity well, which makes rs-fMRI a realizable and broadly used method [19]. Studies have also shown that measurement of low frequency fluctuation magnitude has test-retest reliability, so rs-fMRI can be used as a stable brain feature [20], [21].

Functional connectomes is a typical type of rs-fMRI analysis, using Pearson correlation coefficient to measure functional connectivity between spatial brain region pairs [19].Func-

tional connectivity is the temporary correlation between brain regions that share functional properties. Correlation analysis methods like seed-based functional connectivity analysis (SCA) and independent component analysis (ICA) was further derived from [19] to analyze brain functional connectivity [16], [22]. As more and more datasets had been collected, researchers realized the consistency at the level of network topology in functional connectivity [23], [24]. Therefore, attentions gradually transferred from pair-wise functional connectivity analysis to rs-fMRI network evaluation.

2.2 Resting State Networks

Resting state networks (RSNs) are functional brain regions which fluctuate synchronously in resting state, these networks almost cover the whole brain cortex. RSNs have been verified to own prospective clinical value and provide potential biomarkers of diseases [25]. RSNs include dorsal attention network [30], memory network [26], motor network [19], default mode network [23] etc. In 2011, Yeo et al. parcellated brain cortex into seven functional networks: visual network, somatomotor network, default mode network, dorsal attention network, ventral attention network, frontoparietal control network, limbic network [27]. This parcellation was further adopted by neuroimaging processing and analysis software FMRIB Software Library (FSL) (www.fmrib.ox.ac.uk/fsl) toolbox, and broadly used in many studies [28]–[30].

Among RSNs, DMN is first identified by Raichle et al. [23]. DMN is composed of PCC, medial prefrontal cortex (MPFC) and angular gyrus (AG), where PCC is the central and prominent node of DMN at resting state [31]. MPFC is highly related to mental status and connections between MPFC and PCC differ in distinct social circumstances [32]. AG is a network hub across three separable network modules, thus attention, semantic processing and many other functions are affecting connection around [33]. Even while participants imagine performing music, modulation of functional connectivity near AG can be observed [34]. However, these performances are obvious while doing task-based experiments, so it is difficult for them to influence our resting-state imaging result when participants are healthy individuals.

DMN at rest can be affected by factors like aging and brain concussions. Normal aging would make changes to DMN functional connectivity, studies have shown that part of intrinsic brain functional activity inside DMN would be more intense for younger than elderly subjects [35], [36]. The age difference between middle school players and high school players of our dataset are not that obvious as in previous studies, but the assumption of various functional connectivity performance is still reasonable. For brain concussions, DMN functional connectivity can be affected by asymptomatic HAEs across one season of competition [16].

2.3 Seed based Functional Connectivity Analysis

SCA is a effective and robust functional connectivity analysis method [37]. SCA has also been collected as one module of the Functional Connectivity Toolbox CONN (http://www.conn-toolbox.org), which is a widely used functional connectivity analysis tool. It has been used to successfully detect functional connectivity properties of many seed regions including posterior insula [38], PCC [39], anterior cingulate cortex (ACC) [40]. For example, SCA based on PCC is able to observe functional connectivity changes around DMN [39].

The process of SCA is correlating time series of functional connectivity of selected seed brain region (such as ROI or a special voxel) with that of the whole brain, highly correlated result represents coherent time series of two regions. We can get straight answer of whether one region or voxel is strongly bounded with the selected seed or not from SCA, which is a great benefit to setup some clinical problems [41]. SCA and ICA are two widely used method to analyze rs-fMRI and valuable results have been generated [16], [22]. Compared to another typical analysis method ICA , which separates cortex into independent spatial components based on time course correlation [42], SCA is also beneficial because of its low cost and complexity.

One property of SCA is that two coactivating brain networks would confound the boundary of networks recognized, connectivity of any synchronous voxels pairs is irrelevant to which brain network they belong to [43]. Therefore, the clusters SCA detected are not the same concept as functional networks, seed-based region is a temporary brain network centered at seed region. So instead of a strict DMN region, seed-based region of SCA using PCC as

seed is a local brain connections area around the central node of DMN. How much difference between PCC seed-based region and DMN depends on characteristics of the target group. Extremely large deviation would lead to abnormal brain function.

2.4 The Identifiability Matrix

The identifiability matrix, also called the similarity matrix in some studies [44], [45], is another functional connectivity analysis method. It is a reliable way to measure the extent of identification of functional connectivity variation in some brain regions [46]. The word "identification" means individuals can be accurately identified from a group using functional connectivity changing pattern. In other words, some functional connectivity profiles can be regarded as "fingerprint" of a subject group. Many studies have shown that functional connectome is a reliable individual brain fingerprinting which can keep stable for years, the robustness is verified using several fMRI datasets including healthy people and patients [46], [47].

The identifiability matrix is generated from functional connectivity of specific brain regions of two scans, measuring functional connectivity correlation between each other. The brain region can be one ROI, one functional network or the whole brain, depending on which participant group we focus on. Both functional connectivity alteration between two sessions and between task-based and resting state scans can be used as identification. Identifiability matrix between sessions measures consistency of functional connectivity in certain period of time, for example, [46] exhibited test-rest reliability using high identification between resting sessions.

There are many ways to evaluate identification from the identifiability matrix. If we pick peak correlation coefficient as predicted identity, use binary scores to evaluate identification, then the final score would determine the success rate of identification. Based on this measurement, the differential identifiability matrix was proposed by Amico et al. in 2018 [48]. We can also compare diagonal values of identifiability matrix with mean value of off-diagonal elements, difference between them manifests identification level of the group [17].

Further, identification can be enhanced by reorienting the identifiability matrix, such as using principal component analysis (PCA) [17], [48]. Stronger fingerprint can be extracted from functional connectivity.

2.5 Repetitive HAEs

Functional connectivity analysis methods mentioned in previous sections helps investigating the impacts of HAEs. Changes in brain functional connectivity across the season of competition can be observed using rs-fMRI [49]–[51]. With SCA, significant decrease also exists in functional connectivity of the highly correlated regions with ACC and PCC of athletes compared to peer controls [52]. Since rs-fMRI analysis methods are effective ways to measure the impact of HAEs, we would expected to see some properties related to repetitive HAEs in rs-fMRI analysis.

The reason why repetitive HAEs is important is that brain damage from HAEs turns out to be cumulative [10]–[12]. The long term influence of HAEs to young football players, especially those who exposed to this sport in very young age, can be severe [53]. Even for high school players, accumulative property can be proved by analysis of biomechanical data [12]. So not only the HAE intensity, but also the count of HAEs matters for potential brain injuries.

There were many studies focus on influence of different magnitude of HAEs. The xPatch (X2 Biosystems, Seattle, WA) is an effectively monitor for acceleration while football players receive blows. Peak linear acceleration (PLA) is a good indicator for the magnitude of HAEs. Research has shown that those have PLA larger than 80g would be regarded as high intensity concussive motions [54]. High magnitude HAEs can be highly related to cerebrovascular reactivity [55]. While for lower intensity HAEs, different impairment was observed by clinician and by functional analysis while PLA varies in the range of 15g to 150g [10], so brain connectivity performance varies in player group receiving subsets of HAEs with different PLA magnitude. About the range of PLA, some studies have shown that the average PLA for young athletes is 62.4g$\pm$29.7g, which is much lower than adult athletes [56]. Thus, the statistics can be even lower for middle and high school players instead of professional athletes.

3. METHODS

3.1 Participants

Participants of this study were football players and peer controls in US. middle school and high school, male students in age 12-18. Each individual was scanned once before season and once after season. There are 11 middle school football players and 2 middle school non-collision controls, who were in 12-14 years old. 6 of the players were 8th grade students (mean=13.5) and the other 5 players were in 7th grade (mean=12.6). Controls were both in 8th grade. High school students include 15 football players and 9 controls. Players were from 15 to 18 years old (mean=16.6), 8 of them in 15-16 years old (mean=15.9) and the others in 17-18 years old (mean=17.4). Controls were from 14 to 18 years old (mean=16.1).

3.2 Data collection

All of the participants were scanned before and after one season by a GE Discovery MR750 3T Scanner located at the Purdue MRI facility. T1 and T2-star weighted images generated from an Echo-Planar Imaging (EPI) sequence were stored as Digital Imaging and Communications in Medicine (DICOM) files. T1 structural images were 1mm isotropic and TR were 5.7msec. T2-star images were assigned a 3.8mm slice thickness, a field-of-view (FOV) of 3.125mm×3.125mm and TR of 2sec. The number of time points of the T2-star images were 294 for high school students and 240 for middle school students. In this study, we used T2-star images to achieve functional MRI.

Players wore an xPatch sensor which attached to their head (behind their right ear) during each practice and game to monitor the impacts that they received. Data of HAEs were then collected from the Head Impact Monitoring System software (X2 Biosystems; Seattle, WA), including PLA data. Any acceleration event with PLA above 20g was recorded.

3.3 Data processing pipeline

Data processing of rs-fMRI images relied on Analysis of Functional NeuroImages (AFNI) and FSL. The overall processing pipeline was coded in MATLAB and proposed in [17]. This pipeline can be divided into three steps.

The first step is registration of gray matter (GM) in T1 brain images. We used the FSL anatomical processor *fsl_anat* to do bias correlation and first step registration. Then the Marker Based WaterShed Scalper toolbox (MBWSS) [57] was used to extract the brain from the skull. Individual brain images were aligned with the MNI space and used the same transformation to align with the shen278 parcellation [58], the yeo7 parcellation [27], and the left and right PCC regions. Images went through further intensity normalization with AFNI 3dUnifize, and then the GM was extracted using FSL FAST.

The second step is processing rs-fMRI BOLD images based on T1 templates. Because for each object measurement, there are several bad scans at the beginning before tissue's magnetization goes to a steady state [59]. The artefacts due to the wrong position history of objects are called spin-history artefacts. To remove the effects of spin history, we deleted the initial 4 volumes from each BOLD timeseries, so that the final volumes of the middle school rs-fMRI scans were 236 and the volumes of the high school scans were 290. rs-fMRI images went through outlier detection, despiking and slice timing correction using AFNI functions and then were registered to volumes with minimal outliers. Based on the T1 images from step one, the rs-fMRI timeseries were warped to the MNI template. Then we added a GM mask to rs-fMRI images and did spatial smoothing with a 4mm full-width-at-half-maximum (FWHM) Gaussian kernel. We then scaled the BOLD timeseries and removed any volumes with motion derivative norms over 0.4. The GM timeseries was then divided into the shen278 ROIs, which is a basic parcellation of the brain. Because part of the cerebellum was not covered in scans initially, we removed the 42 ROIs within the cerebellum to keep the result consistent so that the number of ROIs totaled 236.

The last step is functional connectivity matrix calculation from the averaged value of each region of rs-fMRI parcellation. This part was modified from the pipeline designed by [17] in that seed-based analysis were also added. By cross correlating the mean timeseries of

all 236 ROIs of rs-fMRI, we generated a 236*236 functional connectivity matrix. The matrix is symmetric since changing the order of a ROI pair does not change the correlation value between them.

3.4 Data analysis

3.4.1 Consistency and identification analysis

In order to compare pre-season and post-season functional connectivity, identifiability matrices are generated from functional connectivity matrices. Because functional connectivity matrices are symmetric, upper triangular elements are enough to represent connection between all ROI pairs. We transformed upper triangular values to vector and correlated pre-season vector with post-season vector, we finally calculated 13 by 13 identifiability matrix for middle school participants and 24 by 24 matrix for high school group. Diagonal values of identifiability matrices are inter-person functional connectivity correlation value across the season and non-diagonal values are correlation value between pre-season scan of one person and post-season scan of another.

Identifiability difference (I_{diff}) is a value to measure how much difference is between diagonal values and non-diagonal values, which manifests identification. While self-identifiability (I_{self}) value represents diagonal values and indicates consistency of functional connectivity across the season [17].

$$I_{self}(k) = I_{kk}, \forall k = 1, 2, ..., N \tag{3.1}$$

$$I_{others}(k) = \frac{1}{N-1}\sum_{\mathrm{i}\neq k} I_{\mathrm{i}k} + \frac{1}{N-1}\sum_{\mathrm{i}\neq k} I_{k\mathrm{i}}, \forall k = 1, 2, ..., N \tag{3.2}$$

$$I_{diff}(k) = I_{self}(k) - I_{others}(k), \forall k = 1, 2, ..., N \tag{3.3}$$

The higher I_{diff} values are, the stronger difference is between inter-subject correlation and cross-subject correlation. The higher I_{self} value is, the more consistent functional connectivity is across the season.

3.4.2 Yeo resting state networks analysis

As seven RSNs proposed by Yeo et al. are generated from the parcellation based on intrinsic brain connectivity [27], We used the identifiability matrix based on intrinsic functional connectivity of each RSN to measure the identification of individuals of our participant group. Because the network models are not generated from our dataset, potential parcellation deviation might exists. The seven networks are visual network, somatomotor network, dorsal attention network, ventral attention network, limbic network, frontoparietal control network and DMN, and their sizes are respectively 26, 33, 22, 19, 13, 33, 54 ROIs after mapping to 236 regions. As we can see, DMN is the largest network of all.

The I_{diff} value of each identifiability matrix for 7 networks indicates whether the inter-subject functional connectivity correlation of players are higher than cross-subject correlation across the season of play, identification (or "fingerprinting") based on each RSN could be different for middle school and high school football players.

Variation ratio is defined as the percentage of increase from the mean I_{diff} of middle school players to that of high school players.

$$variation\ ratio\ = \frac{high\ school\ I_{diff} - middle\ school\ I_{diff}}{middle\ school\ I_{diff}}$$

The higher variation ratio is, the larger increase exists from middle school player group identification to high school player group identification. If variation ratio is negative, then identification decrease from middle school to high school.

3.4.3 Seed based region of interests

Then we focus on DMN and analyze how the intrinsic functional connectivity change across the season base on our dataset. The performance is more adaptive to our participant group than the DMN analysis in the previous section.

We fist picked 5mm radius circular region at both left and right PCC as seed ROI, and then by correlating the seed ROI with all the 236 ROIs, we picked the ROIs highly correlated with two seeds at the same time ($p<0.05$) for each player's pre-season session, which is called

seed-based ROIs for each subject. Changes of seed-based ROIs between pre-season scan and post-season scan could reveal the influence of concussion in players.

For SCA, we would only consider about the highly correlated region with seed for the entire group. However, from the map of common highly correlated ROIs for all players which indicates a common brain functional connectivity network around PCC of the group, we would get a very small number of ROIs in the map. Because our aim is to find a more general correlation region with PCC instead of strictly limit ROIs to be the common correlated region for every player, we relax the limitation to common correlated ROIs for some of the players. From the relation of the threshold of player count and the number of common highly correlated ROIs among the certain number of players, we picked a point at around the middle of descent curve and set a threshold for the player number. As is shown in Figure3.1, the x-axis is the number of players. If x is 5, then corresponding y value is the number of ROIs correlated with seed for 5 players at the same time. There are 11 middle school players and the number of highly correlated ROI is decreasing since x is larger than 3. We pick the middle of this decreasing slope as our threshold which is 6, so that the seed-based ROIs are highly correlated with seed for most of the players but not everyone.

The threshold we picked is 6 out of 11 middle school players and 9 out of 15 high school players. If the ROI is the common highly correlated ROI over the threshold number of players and is correlated to both left and right PCC, then we mark it as seed based ROI for the group. The final number of seed based ROIs is 150 for middle school group and 170 for high school group. Seed-based functional connectivity matrix is generated from cross correlation value of these seed based ROIs, diagonal elements are self correlation of ROIs which are all 1, and off diagonal values are correlation between two ROIs. Seed-based functional connectivity matrix is also symmetric.

Further three subsections are all analysis methods based on the seed-based functional connectivity matrix.

3.4.4 ICC analysis

Intraclass correlation coefficient (ICC) is a statistical model to assess measurement of reliability, the basic concept is evaluating reliability of observations on objects from different

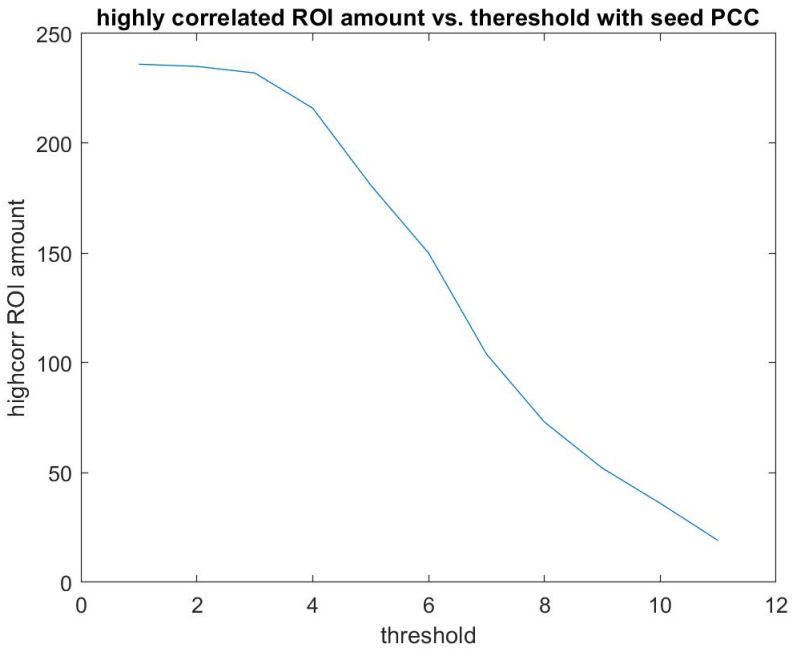

Figure 3.1. Middle School seed based ROI count and the threshold of player count. If x is 5, then corresponding y value is the number of ROIs correlated with seed for 5 players at the same time.

judges [60]. ICC analysis has been used in fMRI to evaluate test-retest reliability on brain functional activations, where we treated functional connectivity as the observation, test and retest as two judges and measure whether judges make reliable observations for all the participants. ICC successfully provided evidence for fMRI reproducibility [61].

Though ICC is also called correlation coefficient, it is different from the Pearson correlation we used in functional connectivity matrix. The difference between the two is that Pearson's r manifests stability of voxel activation compared to other voxels, ICC shows stability of individual session activation compared to other individuals in the group [62].

While applying to SCA, we regarded functional connectivity of seed based ROIs as the observations and players as the objects, ICC analysis gave an assessment on seed-based region functional connectivity variation from pre-season to post-season [17]. Result of ICC model is called ICC matrix, which is in the same dimension as functional connectivity matrix. The higher value corresponding to the lower group difference for the changes in each ROI across the season. This analysis bases on MATLAB ICC model proposed by [63].

3.4.5 Seed-based identification analysis

The second analysis on seed-based functional connectivity matrix is identification analysis. Similar to the identifiability matrices calculated in section 3.4.2 for Yeo networks, we would generate a 13 by 13 matrix from middle school data and a 24 by 24 matrix from high school data for PCC seed-based region too. By here we need to do a quality control further.

As we mentioned in section 3.4.1, the higher I_{diff} values are, the stronger difference is between inter-subject correlation and cross-subject correlation. If diagonal value in identifiability matrix is lower than the mean of non-diagonal values for a particular row/column or subject, then that means functional connectivity of post-season scan of this person is more similar to that of other individual's pre-season scan than that of himself [44]. This individual can not be identified from the group. If this abnormal situation happens, we would assume that there are some errors in the time series of pre-season scan of this participant and remove this sample from the dataset. The 13 participants of middle school and 24 participants of high school mentioned are good quality samples after quality check, in total 2 high school samples (one player and one control) are discarded during this step.

Age difference is expected to be observed in I_{self} values. Here we have five groups: controls, 7th grade middle school players, 8th grade middle school players, 15-16 years old high school players and 17-18 years old high school players. Because we have a small number of data and no experimental I_{self} probability distribution is given, only non-parametric statistic test can be used. Kruskal-Wallis test is similar to one way ANOVA (parametric method), it tests null hypothesis for several independent groups. Here we used it to compare distribution of I_{self} between controls (baseline) and other player groups. Given the null hypothesis that two sample groups come from the same distribution, if p value is smaller than significance value 0.05, then the null hypothesis can be rejected. Kruskal-Wallis test is based on MATLAB function.

3.4.6 PLA data analysis

PLA data analysis is based on the seed-based identifiability matrix. I_{self} is a measurement of functional connectivity consistency of subjects across the season of play and we

made an assumption that functional connectivity consistency is negatively correlated with the intensity of HAEs. The magnitude of HAEs is quantified by PLA, each player has a corresponding PLA data from the xPatch sensor along the season. Every acceleration with PLA larger than 20g is recorded. Since we want to analysis a wide range of accelerations, we considered the subsets of HAEs with PLA larger than 20g, 30g, 40g, 50g, 60g, 70g and counted the number of events in these ranges. The data shows that how many light HAEs and heavy HAEs did the players receive in practices and games during the season of play. A scatter plot of HAE counts of 6 subsets with different PLA thresholds and I_{self} directly pictures the relation between HAEs acceleration data and functional connectivity consistency, and we try to validate our hypothesis with the distribution.

4. RESULTS

Table 4.1 and 4.2 present middle school and high school in-network identifiability matrices. The reason why it is called "in-network" is that we picked the intrinsic ROIs of each Yeo network and then generated corresponding functional connectivity matrices and identifiability matrices. I_{self} and I_{diff} values indicate the inter-subject and cross-subject correlation of connectivity each network between pre-season and post-season scans. Here we use the general model of 7 functional resting-state networks to compare the performance with each other [27].

The seven Yeo networks respectively are visual network, somatomotor network, dorsal attention network, ventral attention network, limbic network, frontoparietal network and default mode network. The number of ROI of each network is 26, 33, 22, 19, 13, 33, 54. The comparison of mean I_{diff} value of the seven networks between middle school players and high school players is shown in Figure 4.1.

However, one network of them is of bad quality for our dataset. Yeo5 is not only the smallest one but also the most blurring part of rs-fMRI images. Many young subjects wear brace which blocked the signal for almost half of the region of yeo5. Therefore it has a corresponding lowest I_{diff} (Figure 4.9) and we can hardly see diagonal feature in Table 4.3 first line. As to its bad data quality, further Table 4.4 would skip yeo5 (Limbic network).

Table 4.1. Middle school and high school in-network identifiability matrix yeo1 to yeo4

Network name	middle school	high school
visual network (yeo1)	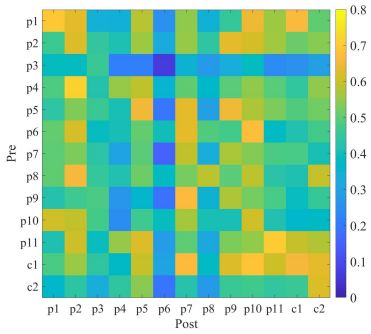	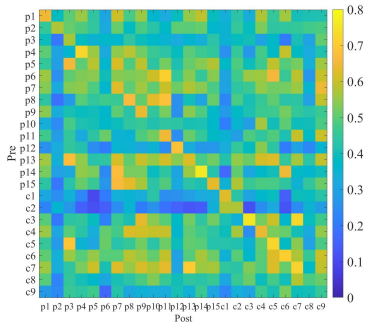
somatomotor network (yeo2)	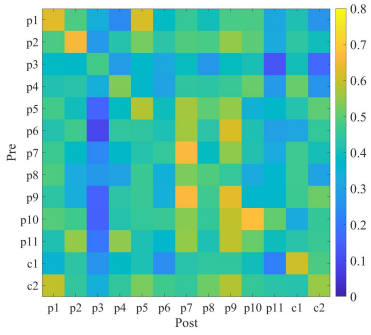	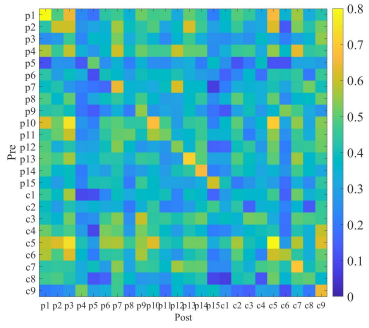
dorsal attention network (yeo3)	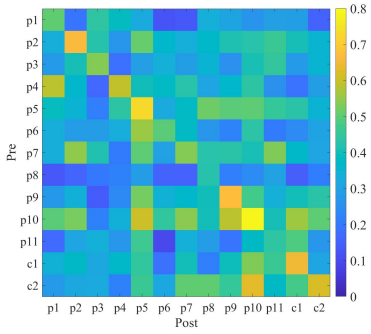	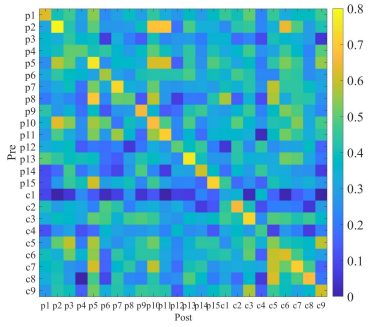
ventral attention network (yeo4)	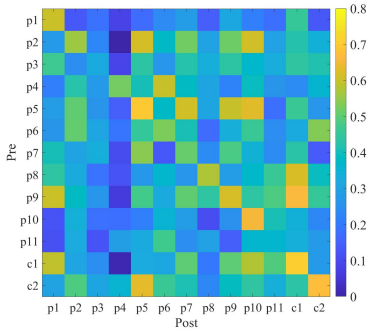	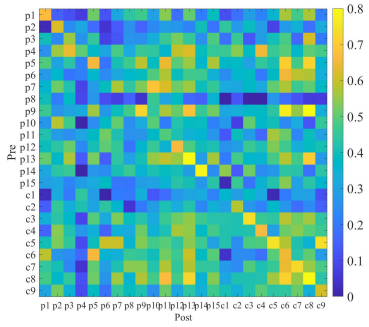

Table 4.2. Middle school and high school in-network identifiability matrix yeo5 to yeo7

Network name	middle school	high school
limbic network (yeo5)	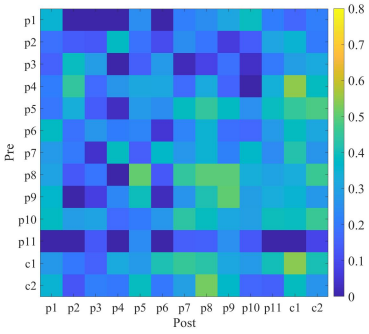	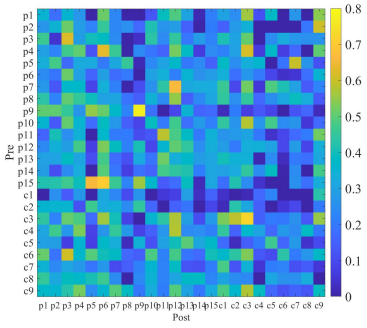
frontoparietal network (yeo6)	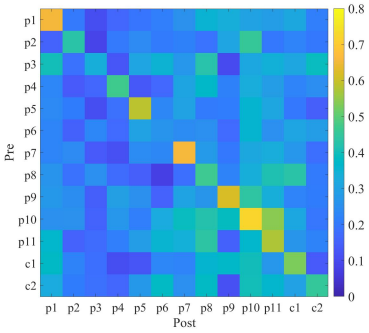	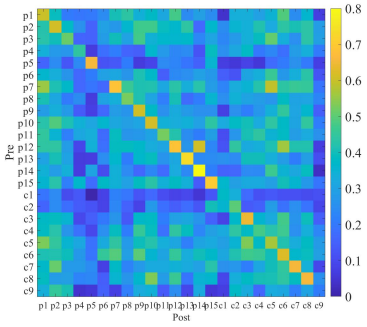
default mode network (yeo7)	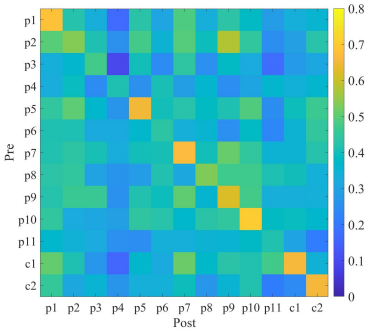	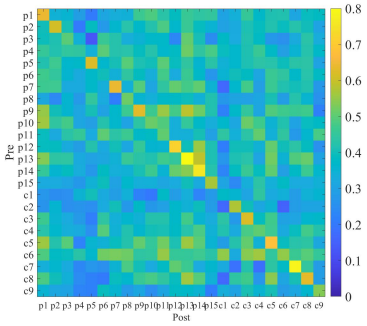

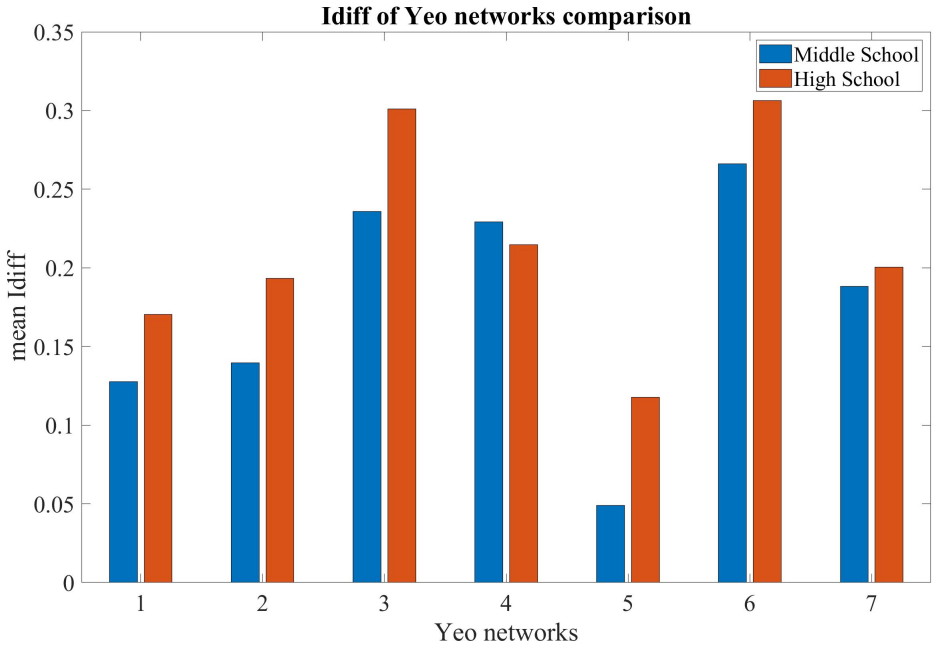

Figure 4.1. Yeo identifiability matrices I_{diff} comparison between middle school and high school players

Table 4.3 indicates the variation ratio, which is the percentage of increase from middle school mean I_{diff} to high school mean I_{diff}, of six Yeo networks. We can observe different variation from middle school to high school of these networks.

Table 4.3. Variation ratio of six Yeo networks. Variation ratio represents percentage of increase from middle school mean I_{diff} to high school mean I_{diff}.

Yeo network	visual	somatomotor	dorsal attention	ventral attention	frontoparietal	DMN
variation ratio(%)	33.36	38.44	27.60	-6.35	15.12	6.50

Further result figures and tables are related to seed-based functional connectivity. the ROIs that highly correlated with seed region (PCC) for all players are shown in the following map. The grey background of Figure 4.2 and 4.3 is a parcellation of GM (shen278 parcellation [58]), in total 278 ROIs. The yellow regions are DMN mask and the red regions are ROIs that highly correlated with PCC (here we call the red region as seed-based map).

The seed-based map is different from the region which seed-based functional connectivity matrices based on, because functional connectivity matrices need to be a more general case and include more possibly related connections. Here we mapped the common ROI region of all players in order to view the intersection of seed-based functional connectivity of this player group. Abnormal group intrinsic DMN functional connectivity could be found if we compare it with the commonly used DMN map.

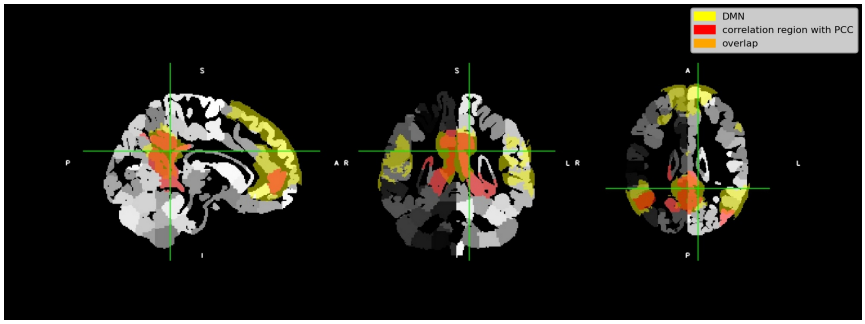

(a) Middle school pre-season seed-based map

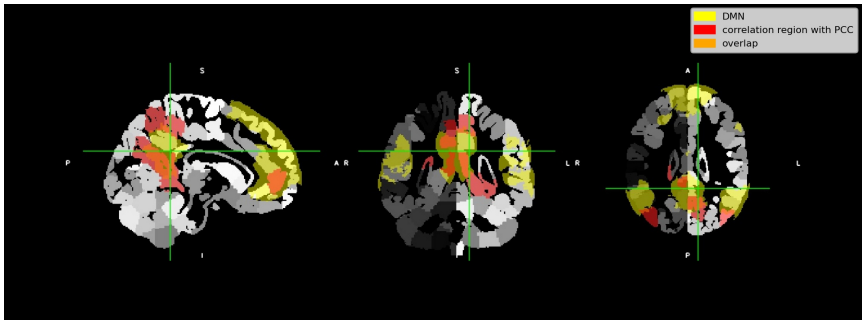

(b) Middle school post-season seed-based map

Figure 4.2. Yellow regions are DMN network and red regions are ROIs highly correlated with PCC for all players ($p<0.05$). Grey background is shen278 parcellations and there are 278 ROIs with different grey level. (a): there are 16 ROIs in red regions, 10 overlap with the DMN mask(yellow regions); (b): there are 14 ROIs in red regions, 7 overlap with DMN mask(yellow regions). There are 6 different ROIs between pre-season and post-season seed-based maps.

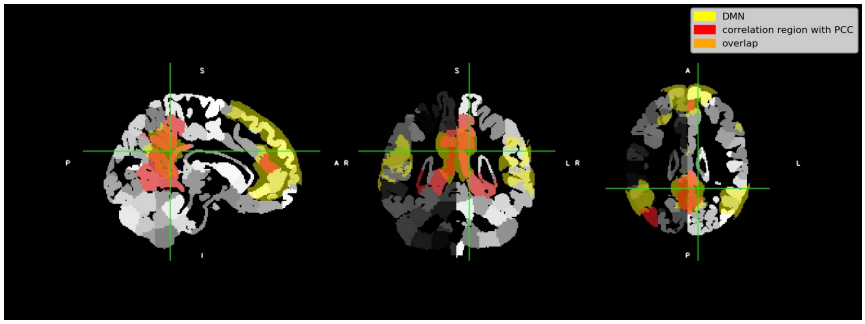

(a) High school pre-season seed-based map)

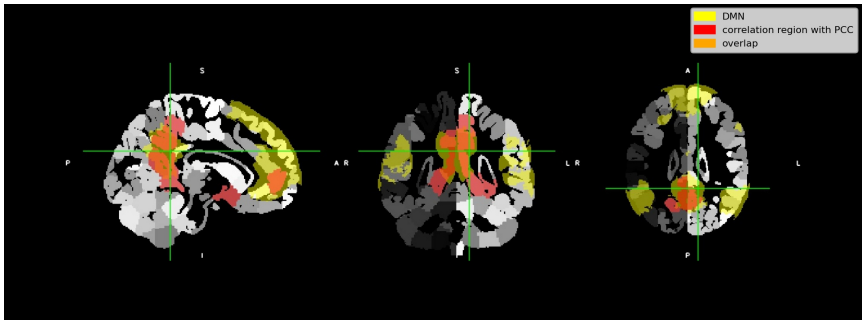

(b) High school post-season seed-based map

Figure 4.3. Yellow regions are DMN network and red regions are ROIs highly correlated with PCC for all players ($p<0.05$). Grey background is shen278 parcellations and there are 278 ROIs with different grey level. (a): there are 18 ROIs in red regions, 11 overlap with the DMN mask(yellow regions); (b): there are 18 ROIs in red regions, 11 overlap with DMN mask(yellow regions). There are 5 different ROIs between pre-season and post-season seed-based maps.

ICC matrices of high school players and controls are shown in Figure 4.4 to compare functional connectivity test-retest reliability of players with controls. Because we only have 2 middle school controls, the number of controls is not comparable with middle school players. Therefore, high school participants are observed in this part.

Each pixel indicates test-retest reliability of functional connectivity within one ROI pair (236 ROIs in total, mentioned in methods3.3). As diagonal values are corresponding to connectivity between ROIs and themselves, diagonal values of ICC matrices are all 1. Besides, ICC matrices are symmetric as elements above diagonal correspond to the same ROI pairs as those below diagonal.

In order to see whether there is any feature in ICC matrices, we reduced the range of values in Figure 4.4.

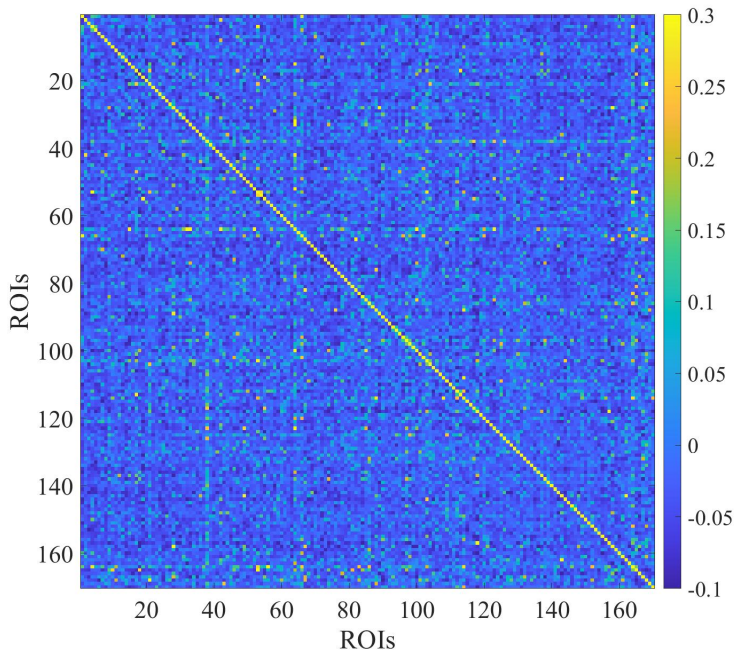

(a) Reducecd range ICC matrix of high school players

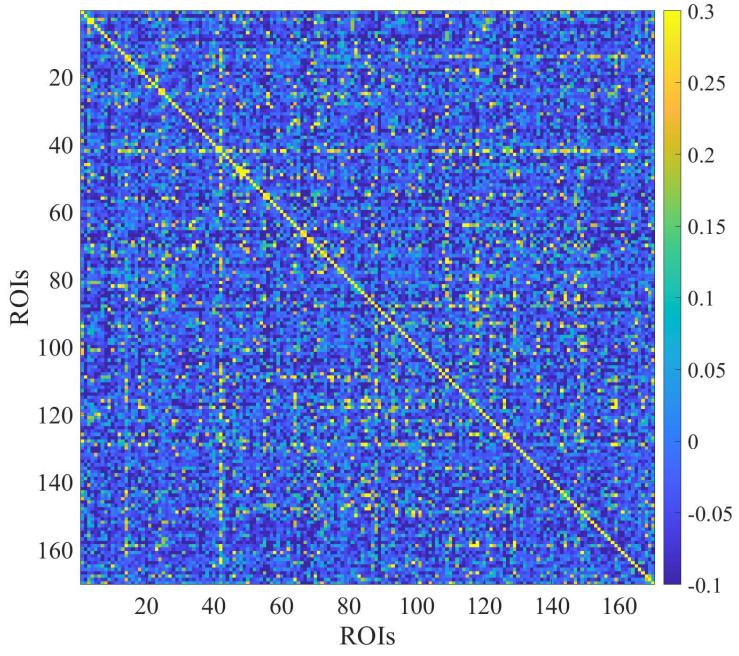

(b) Reduced range ICC matrix of high school controls

Figure 4.4. ICC matrix for high school players(a) and controls(b). Both are reduced to range from -0.1 to 0.3 in order to see detail matrix pattern. Any pixel value larger than 0.3 is marked as yellow, and that smaller than -0.1 is blue here.

Because diagonal values are all 1 and ICC matrices are symmetric, in Figure 4.5, we focused on the upper triangular values and their distribution.

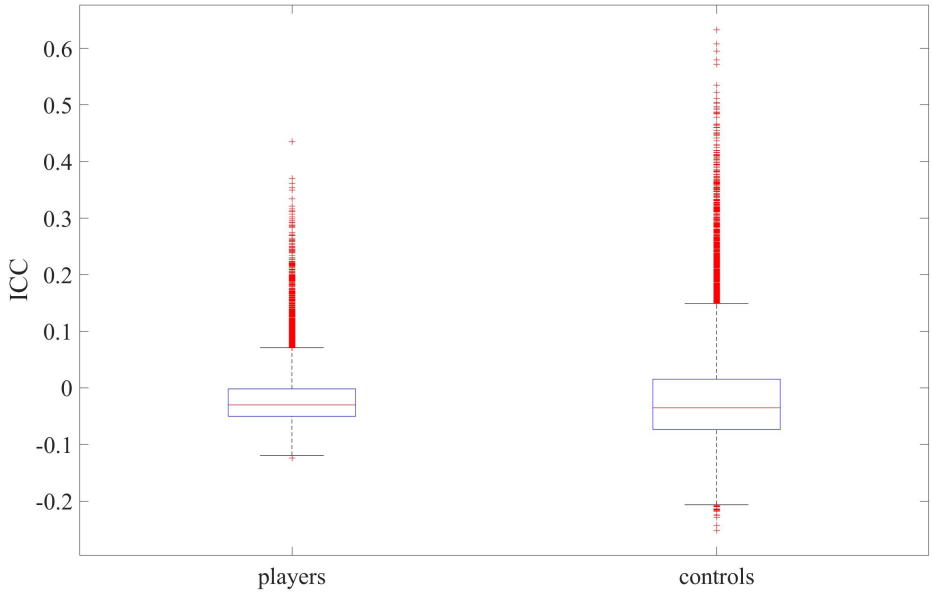

Figure 4.5. Distribution of high school ICC upper triangular values

Figure 4.6 and 4.7 base on the ROIs that highly correlated with seed region PCC, Identifiability matrices show the changes of functional connectivity within these seed-based ROIs across the season. Each element represents correlation value between two scans. Diagonal value represents the across-season changing for each person and off-diagonal values are difference between pre-season scan of one person and post-season scan of another.

I_{diff} indicates difference between inter-subject correlation (diagonal values) and cross-subject correlation (off-diagonal values), also manifests whether each individual can be identified from the group using functional connectivity. The identifiability matrix and I_{diff} values of participants are shown in Figure 4.6 (high school) and Figure 4.7 (middle school).

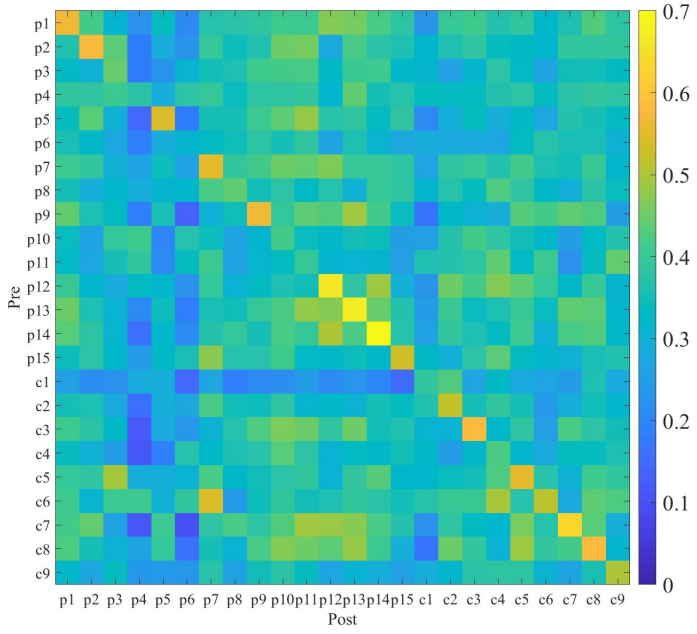

(a) High School seed-based identifiability matrix

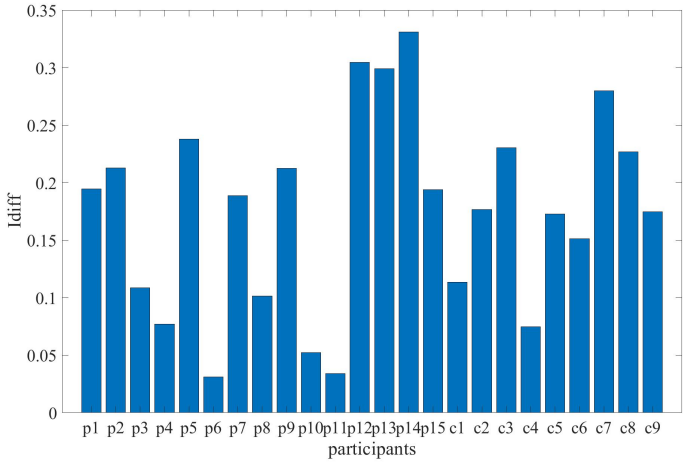

(b) I_{diff}

Figure 4.6. High school seed-based identifiability matrix (a) and I_{diff} (b). (a): this matrix is a similarity comparison of post-season scan with pre-season scan. The horizontal axis represent post-season scans and the vertical axis represent pre-season scans. Rows and columns labeled with p are players, with c are controls. In total 15 players and 9 controls.

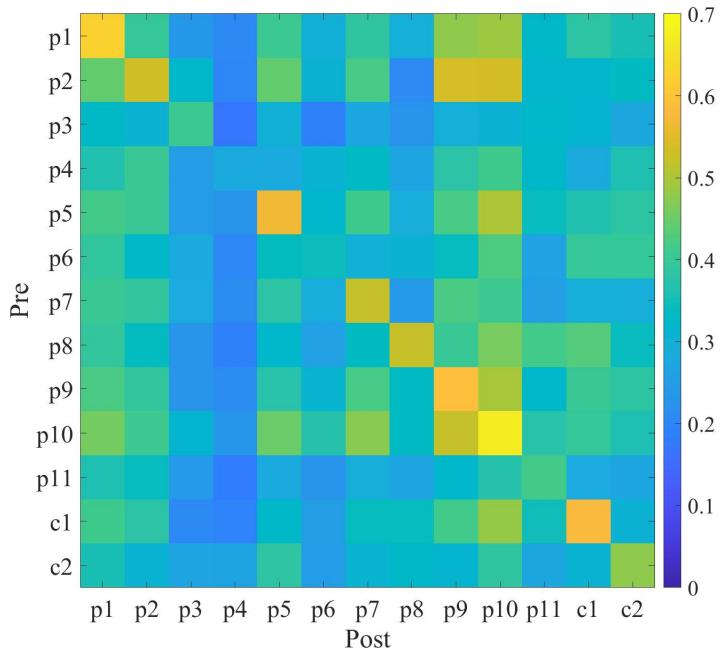

(a) Middle school seed-based identifiability matrix

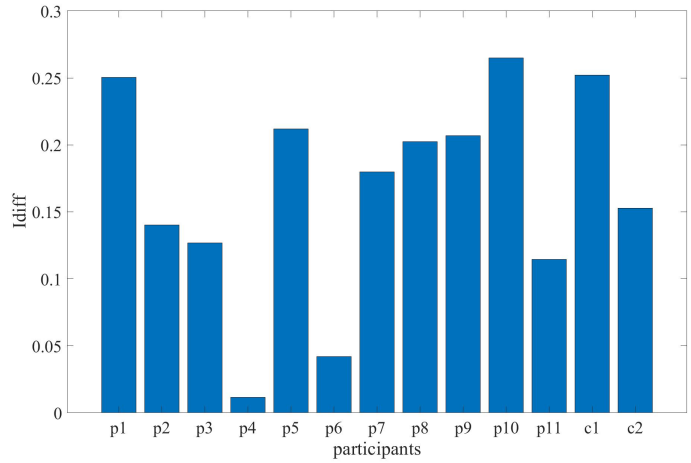

(b) I_{diff} values

Figure 4.7. Middle school seed-based identifiability matrix (a) and I_{diff} (b). In total 11 players and 2 controls

Distribution of diagonal value of identifiability matrices is shown in Figure 4.8. Here we seperated all participants into 5 groups: controls of middle school and high school, middle school 7th grade players, middle school 8th grade players, high school 15-16 years old players and high school 17-18 years old players. The distribution of all groups is statistically equivalent. Table 4.4 proves the equivalence using Kruskal-Wallis test.

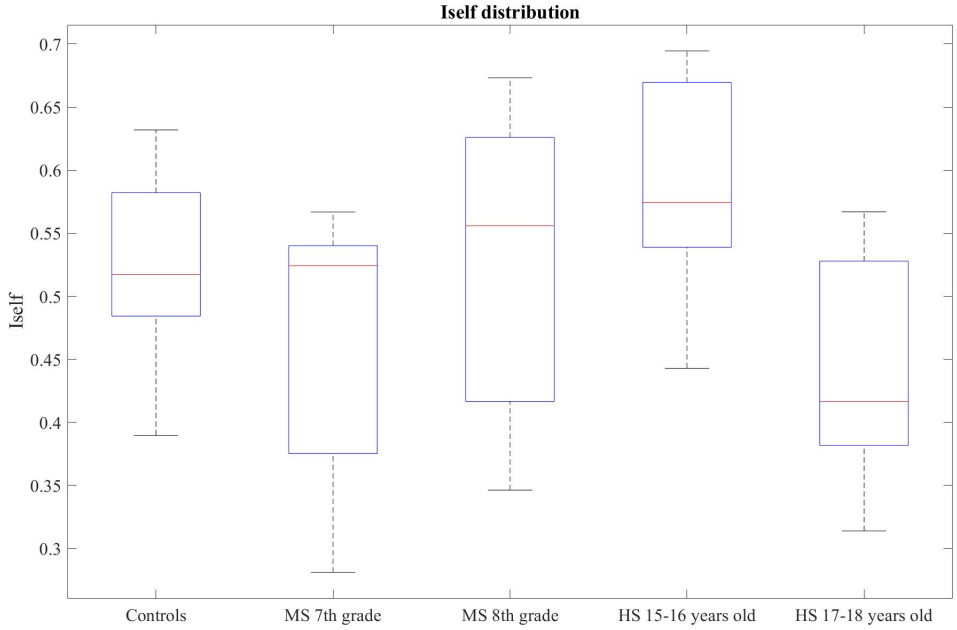

Figure 4.8. Boxplot distribution of I_{self} in Figure 4.5 and 4.6. The five groups here are controls of middle school and high school, middle school 7th grade players, middle school 8th grade players, high school 15-16 years old players and high school 17-18 years old players

Table 4.4. Kruskal-Wallis test between I_{self} values in identifiability matrix of control group and that of other player groups in Figure 4.7

KW test (with controls group)	middle school 7th grade	middle school 8th grade	high school 15-16 years old	high school 17-18 years old
p value	0.6917	0.6877	0.6203	0.5561

Figure 4.9 scatter plots show the relation between count of events with PLA larger than 20g, 30g, 40g, 50g, 60g, 70g and I_{self} of seed-based identifiability matrix.

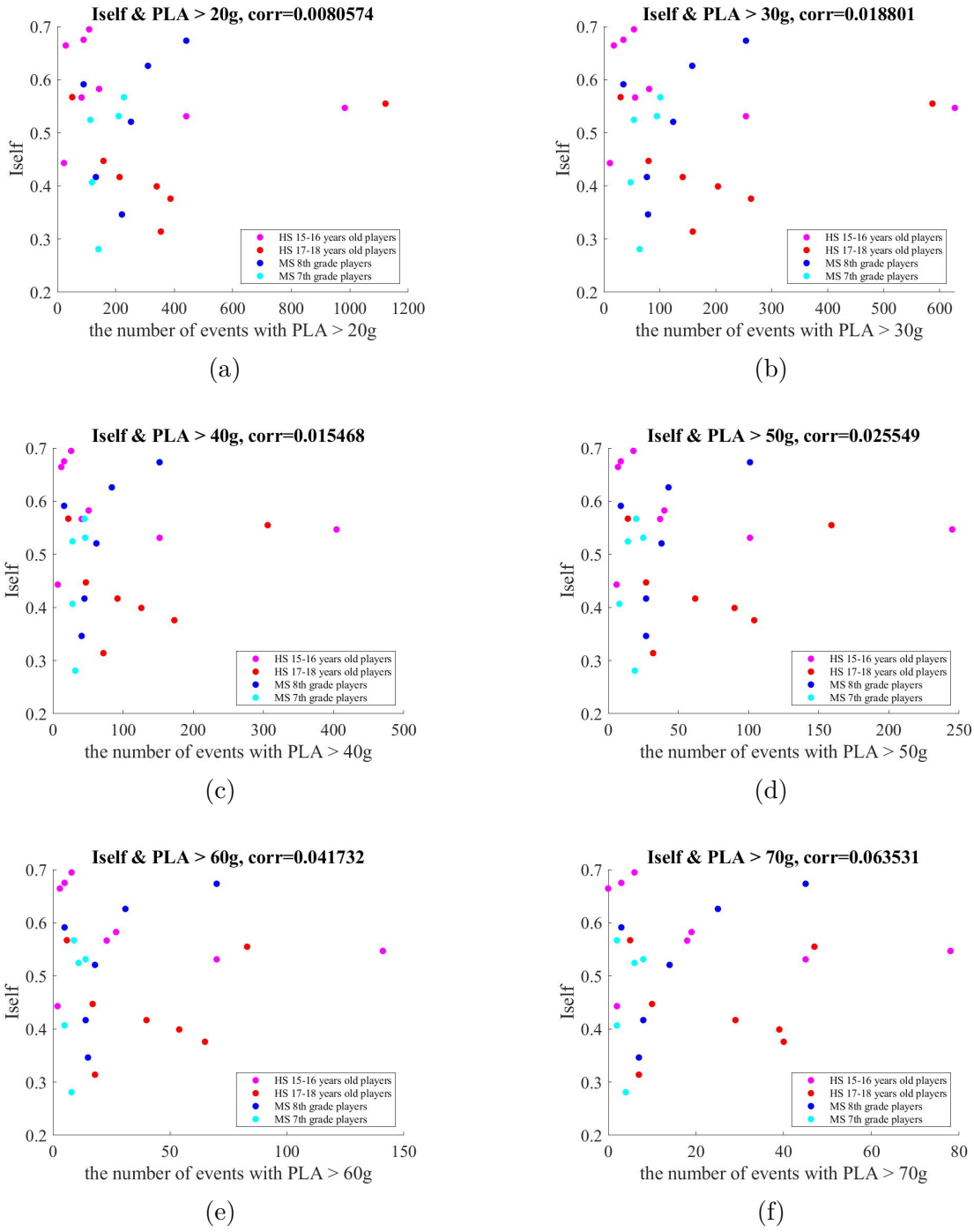

Figure 4.9. Count of events exceeding the indicated acceleration threshold and I_{self} scatter plot: (a-f) are the distribution of the number of events whose PLA larger than 20g, 30g, 40g, 50g, 60g and 70g. Red dots represent 17-18 years old high school data, magenta dots represent 15-16 years old high school data, blue dots represent 8th grade middle school data and cyan dots represent 7th grade middle school data. Correlation values in the titles are calculated from all the data points in the figure

5. DISCUSSION

5.1 Brief Summary

Brain systems subserve our functions such as memory function, motor function, sensory function and so on. In 2011, Yeo et al. proposed a parcellation of brain cortex based on rs-fMRI and each part is potentially related to some functions [27]. The seven parts represent seven functional brain networks, changes in functional connectivity have been observed in task based fMRI studies related to corresponding cognitive functions [64], [65]. This parcellation has considerable impact on network neuroscience, many studies have used Yeo seven networks as a template [28], [29], [64]. Therefore, we also used that as a template in our study.

For seven Yeo RSNs, in-network identifiability matrices indicate different identification level of each network. Dorsal attention network and frontaprietal network have relatively higher identification, while visual network and somatomotor network have a relatively lower value. The difference between the mean identification of middle school data and that of high school data is also interesting. Identification of somatomotor network has the largest increase from middle school players to high school players, matching with the development of adaptive physical activity skills for young football players.

For SCA on DMN, seed-based ROI maps of middle school group and high school group manifest the influence of age factor on functional connectivity. Post-season highly correlated brain region with PCC is different from that of pre-season, and the change of number and position of seed-based ROIs is larger for middle school players than high school players. Another finding is that ICC analysis on seed-based functional connectivity matrix exhibits a narrower range of individual difference in functional connectivity variation across the season for player group than control group, showing the influence of HAEs.

However, seed-based identifiability matrix turns out not a good indicator for HAEs in our dataset. There is no statistically significant difference in functional connectivity consistency across season between controls and players, which fits for players in different age group. Also, against our hypothesis, functional connectivity consistency is not related to the number of

HAEs received, nor to the intensity of HAEs. Therefore, there is no relation found between HAE counts, intensity and seed-based identifiability matrix.

5.2 Yeo networks identification comparison

Identifiability matrices in Table 4.1 and 4.2 base on ROIs within each brain network and exhibit the consistency and identification of intrinsic network functional connectivity. Seven Yeo networks respectively are visual network, somatomotor network, dorsal attention network, ventral attention network, limbic network, frontoparietal network and default mode network. As to the bad quality of yeo5 network data, further discussion part would skip yeo5 (Limbic network).

From Table 4.1 and 4.2, we have a broadly observation that identifiability matrices of yeo1 and yeo2 network of middle school data do not have a clear diagonal feature compared to the other four networks, this observation get verified in bar plot Figure 4.1. Yeo1 and yeo2 turn out to be the two networks with lowest I_{diff}, and thus post-season visual network and somatomotor network are more likely to resemble others' pre-season scans. While yeo3 and yeo6 have relatively higher I_{diff} values, which is more apparent for high school data, so intrinsic functional connectivity of dorsal attention network, and frontoparietal network are more of the individual brain fingerprints than other networks.

Variation of I_{diff} from middle school to high school data is also different for each network. Statistics in Table 4.3 shows the percentage of I_{diff} variation (how much proportion of variation is in middle school I_{diff}). High school data generally have higher I_{diff} than middle school except for yeo4 (ventral attention network). Ventral attention network identification is weaker for the older group of our dataset. Of the other 5 networks, fingerprinting variation of visual network, somatomotor network and dorsal attention network are relatively stronger. Somatomotor network even has the highest variation proportion among them, which matches with our football player participant group. As players develop adaptive physical skills after repetitive practice, distinct Somatomotor network intrinsic connectivity could also generated during brain maturation.

5.3 Age dependence in seed based ROI

Figure 4.2 and 4.3 are respectively middle school and high school seed-based ROI map. Here we mapped the common ROI region of all players and observed the intersection of seed-based functional connectivity of this player group. We then compared it with the commonly used DMN map to find if there is any abnormal group intrinsic DMN functional connectivity. For both middle school and high school, pre-season and post-season, over half of the seed-based maps overlap with the DMN map. Besides, the DMN map is also from a broad functional network parcellation template [27] and there could be some personal variation for that. Thus, our seed-based maps have no obvious deviation from the DMN map, and intrinsic DMN brain functional connectivity is verified to be in a normal case.

Also apparent difference between pre-season and post-season maps can be observed. The number of ROIs in those seed-based maps are included in the captions of Figure 4.2 and 4.3. For middle school data, there are 3 more ROIs of the pre-season seed-based map overlap with the DMN map than that of the post-season map, in total 6 ROIs are different between pre-season and post-season maps. For high school data, the number of overlap ROIs is the same but in total 5 ROIs are different between pre-season and post-season maps. From the number of overlap ROIs and variation of ROIs, alteration of seed-based ROI region for middle school turns out heavier than for high school. Thus, high school group common seed-based region is more stable than that of middle school group across the season, age dependence is observed.

5.4 HAE influence to ICC

ICC matrix in this study is used to observe the consistency of judgement from different subjects on the variation of functional connectivity of each ROI pairs across the season of play. Or we can say it measures the test-retest reliability of functional connectivity. Because self functional connectivity is always one which is constant, ICC value of diagonal elements also equal one. For off-diagonal elements, the higher ICC number is, the more similar the variation of functional connectivity is across subjects, so the variation is more of a group feature. Low or even negative ICC value suggests that connectivity judgement

among subjects are diverse, the changing law from pre-season to post-season of the functional connectivity is random in this group.

As is shown in Figure 4.4 and 4.5, ICC analysis was performed to high school players and controls separately. Most ICC value is less or close to zero, so most functional connectivity have random variation in high school group. There is hardly any connectivity changes in the similar way across the season for all players, but there are very few reach ICC>0.5 in control group. The wider range of ICC of control group indicates that some brain functional connectivity variations have an increasing individual difference after receiving HAEs, while some others become more of a group feature after receiving HAEs.

Also, Figure 4.4 show reduced range (-0.1 to 0.3) ICC matrices of players and controls, which give a detail view of ICC value distribution. While observing off-diagonal elements, there are obviously more light pixels in control group and the positions of light or high ICC pixels are different for players and controls. The difference in ICC matrices of players and controls enhances the statement that functional connectivity variation across the season is affected by HAEs.

5.5 Identification and consistency measurements for different age group

As is shown in Figure 4.6 and 4.7, seed-based identifiability matrix is the functional connectivity correlation between pre-season and post-season scans. Diagonal elements are Pearson's correlation between pre-season and post-season scan of the same individual, which we called I_{self}. As diagonal values show the consistency of self seed-based region correlation, I_{diff} values manifest how much functional connectivity similarity between post-season scan and pre-season scan of himself is higher than similarity between post-season scan and pre-season scan of others.

From subfigure (b) of the two figures, I_{diff} values of high school participants are in the range of 0.03 to 0.33 and that of middle school participants are in the range of 0.01 to 0.27. This I_{diff} range matches with the statistics in other research [17]. Subjects like high school p6, p10, p11 and middle school p4, p6 have I_{diff} lower than 0.05, which shows that their post-season scans are similar to pre-season scans of other individual. This is a normal case due to small individual difference while taking one of the scans.

Distribution of middle school and high school I_{self} is shown in Figure 4.8, the higher value I_{self} is the more consistent seed-based ROI functional connectivity is in the season. Five groups here are control group including controls of middle school and high school, and players in middle school 7th grade, middle school 8th grade, 15-16 years old (high school) and 17-18 years old (high school). Since controls have not received any impacts, we could use the first group as a baseline to discuss how sub-concussions are influencing functional connectivity alteration. Middle school 8th grade player group has a wider range of I_{self} than controls, while the other three groups have lower or higher I_{self} range than controls. But the median value of the four groups are close to each other, so we further do statistical test to quantify group difference.

Non-parametric Kruskal-Wallis test (Table 4.4) is used to compare distribution of I_{self} between controls (baseline) and other player groups. Null hypothesis is that two sample groups come from the same distribution. Since significance value is 0.05, all the p values larger than that and are not able to reject null hypothesis. Therefore, seed-based functional connectivity consistency of player groups in different age are not statistically significantly different from that of controls.

5.6 PLA related hypothesis

Figure 4.9 describes the distribution of I_{self} value and the number of events with 6 different PLA thresholds. From the correlation values in titles of figures, we can find a general weak relation between number of HAEs and I_{self} for all six figures. High school data includes two players who received extremely large number of acceleration events. Count of events and I_{self} values of player groups are in the similar range as that of control group. 7th grade middle school players experienced the smallest number of acceleration events.

Originally, our hypothesize is that players with high PLA would have low I_{self} since HAEs gradually disorder functional connectivity between nodes. However, two high school players who received high count of acceleration events have pretty high I_{self} (larger than 0.5) which rejects our hypothesis. One possible explanation of this phenomenon is that players who experienced a large number of HAEs this season also had gotten many impacts before, so their DMN brain functional connectivity has been altered previously and kept in the stable

condition since. But this hypothesis is not able to be proved based on our dataset. From the report of participants, 4 of the high I_{self} high HAE count players and one of the low I_{self} high HAE count players also received concussions before, but reliability of these information is hard to verify. Besides, we don't have specific data of how many HAEs they received before, so further research is needed to observe the long term changing of HAEs count.

6. CONCLUSION

In this study, the influence of age factor and HAEs to DMN intrinsic functional connectivity of young football players is observed using rs-fMRI seed-based analysis method, where the seed region is PCC which is the central node of DMN. Experiments show that both factors make changes to functional connectivity across the season of play. Two age groups have different performances on seed-based ROI map, the change of number and position of the seed-based ROIs across the season is larger for middle school players than for high school players. Also high school player group has a limited ICC range compared to control group, which shows that HAEs do affect functional connectivity alteration in the season.

Meanwhile, some hypotheses of seed-based identifiability matrix are rejected. Our original assumption is that functional connectivity consistency is negatively correlated with count of HAEs received. However, seed-based identifiability matrix turns out not to be a good indicator for HAEs in our dataset. Consistency and identification of functional connectivity are measured by identifiability matrix. Seed-based ROI region lays in normal identification range. But there is no statistically significant difference in connectivity consistency across season between controls and players (based on Kruskal-Wallis test), which is true for player groups in different age range. Also, against our hypothesis, the consistency is not related to the number of acceleration events received, nor to the intensity of any HAEs subsets. Therefore, there is no relation found between count of HAEs in different intensity HAE subsets and seed-based identifiability matrix.

Besides the SCA results on DMN, identifiability matrices of in-network ROIs indicate the different identification level for seven Yeo networks. Dorsal attention network and frontaprietal network have relativly high identification, while visual network and somatomotor network have a relatively low value. Also, the identification of somatomotor network has the largest increase from middle school players to high school players, matching with the development of adaptive physical activity skills for young football players.

REFERENCES

[1] I. K. Koerte, A. P. Lin, A. Willems, M. Muehlmann, J. Hufschmidt, M. J. Coleman, I. Green, H. Liao, D. F. Tate, E. A. Wilde, O. Pasternak, S. Bouix, Y. Rathi, E. D. Bigler, R. A. Stern, and M. E. Shenton, "A review of neuroimaging findings in repetitive brain trauma," vol. 25, 2015. DOI: 10.1111/bpa.12249.

[2] M. McCrea, T. Hammeke, G. Olsen, P. Leo, and K. Guskiewicz, "Unreported concussion in high school football players: Implications for prevention," *Clinical Journal of Sport Medicine*, vol. 14, 1 2004, ISSN: 1050642X. DOI: 10.1097/00042752-200401000-00003.

[3] J. Cournoyer and B. L. Tripp, "Concussion knowledge in high school football players," *Journal of Athletic Training*, vol. 49, 5 2014, ISSN: 10626050. DOI: 10.4085/1062-6050-49.3.34.

[4] J. E. Bailes, A. L. Petraglia, B. I. Omalu, E. Nauman, and T. Talavage, "Role of subconcussion in repetitive mild traumatic brain injury," *Journal of Neurosurgery*, vol. 119, 5 2013, ISSN: 00223085. DOI: 10.3171/2013.7.JNS121822.

[5] C. C. Giza, J. S. Kutcher, S. Ashwal, J. Barth, T. S. Getchius, G. A. Gioia, G. S. Gronseth, K. Guskiewicz, S. Mandel, G. Manley, D. B. McKeag, D. J. Thurman, and R. Zafonte, "Summary of evidence-based guideline update: Evaluation and management of concussion in sports," *Neurology*, vol. 80, 24 2013, ISSN: 00283878. DOI: 10.1212/WNL.0b013e31828d57dd.

[6] M. Makdissi, G. Davis, B. Jordan, J. Patricios, L. Purcell, and M. Putukian, "Revisiting the modifiers: How should the evaluation and management of acute concussions differ in specific groups?" *British Journal of Sports Medicine*, vol. 47, 5 2013, ISSN: 03063674. DOI: 10.1136/bjsports-2013-092256.

[7] M. R. Lovell and V. Fazio, "Concussion management in the child and adolescent athlete," *Current Sports Medicine Reports*, vol. 7, 1 2008, ISSN: 1537890X. DOI: 10.1097/01.CSMR.0000308671.45558.e2.

[8] C. Foley, A. Gregory, and G. Solomon, "Young age as a modifying factor in sports concussion management: What is the evidence?" *Current Sports Medicine Reports*, vol. 13, 6 2014, ISSN: 15378918. DOI: 10.1249/JSR.0000000000000104.

[9] K. D. B. Foss, W. Yuan, J. A. Diekfuss, J. Leach, W. Meehan, C. A. DiCesare, G. Solomon, D. K. Schneider, J. MacDonald, J. Dudley, N. Cortes, R. Galloway, M. Halstead, G. Walker, and G. D. Myer, "Relative head impact exposure and brain white matter alterations after a single season of competitive football: A pilot comparison of youth versus high school football," *Clinical journal of sport medicine : official journal*

of the Canadian Academy of Sport Medicine, vol. 29, 6 2019, ISSN: 15363724. DOI: 10.1097/JSM.0000000000000753.

[10] E. L. Breedlove, M. Robinson, T. M. Talavage, K. E. Morigaki, U. Yoruk, K. O'Keefe, J. King, L. J. Leverenz, J. W. Gilger, and E. A. Nauman, "Biomechanical correlates of symptomatic and asymptomatic neurophysiological impairment in high school football," *Journal of Biomechanics*, vol. 45, 7 2012, ISSN: 00219290. DOI: 10.1016/j.jbiomech.2012.01.034.

[11] S. P. Broglio, J. T. Eckner, D. Martini, J. J. Sosnoff, J. S. Kutcher, and C. Randolph, "Cumulative head impact burden in high school football," *Journal of Neurotrauma*, vol. 28, 10 2011, ISSN: 08977151. DOI: 10.1089/neu.2011.1825.

[12] J. E. Urban, E. M. Davenport, A. J. Golman, J. A. Maldjian, C. T. Whitlow, A. K. Powers, and J. D. Stitzel, "Head impact exposure in youth football: High school ages 14 to 18 years and cumulative impact analysis," *Annals of Biomedical Engineering*, vol. 41, 12 2013, ISSN: 15739686. DOI: 10.1007/s10439-013-0861-z.

[13] H. Lv, Z. Wang, E. Tong, L. M. Williams, G. Zaharchuk, M. Zeineh, A. N. Goldstein-Piekarski, T. M. Ball, C. Liao, and M. Wintermark, "Resting-state functional mri: Everything that nonexperts have always wanted to know," *American Journal of Neuroradiology*, vol. 39, 8 2018, ISSN: 1936959X. DOI: 10.3174/ajnr.A5527.

[14] M. H. Lee, C. D. Smyser, and J. S. Shimony, "Resting-state fmri: A review of methods and clinical applications," *American Journal of Neuroradiology*, vol. 34, 10 2013, ISSN: 01956108. DOI: 10.3174/ajnr.A3263.

[15] D. C. Zhu, T. Covassin, S. Nogle, S. Doyle, D. Russell, R. L. Pearson, J. Monroe, C. M. Liszewski, J. K. DeMarco, and D. I. Kaufman, "A potential biomarker in sports-related concussion: Brain functional connectivity alteration of the default-mode network measured with longitudinal resting-state fmri over thirty days," *Journal of Neurotrauma*, vol. 32, 5 2015, ISSN: 15579042. DOI: 10.1089/neu.2014.3413.

[16] K. Abbas, T. E. Shenk, V. N. Poole, M. E. Robinson, L. J. Leverenz, E. A. Nauman, and T. M. Talavage, "Effects of repetitive sub-concussive brain injury on the functional connectivity of default mode network in high school football athletes," *Developmental Neuropsychology*, vol. 40, 1 2015, ISSN: 87565641. DOI: 10.1080/87565641.2014.990455.

[17] S. Bari, E. Amico, N. Vike, T. M. Talavage, and J. Goñi, "Uncovering multi-site identifiability based on resting-state functional connectomes," *NeuroImage*, vol. 202, 2019, ISSN: 10959572. DOI: 10.1016/j.neuroimage.2019.06.045.

[18] F. A. Nasrallah, L. Y. Yeow, B. Biswal, and K. H. Chuang, "Dependence of bold signal fluctuation on arterial blood co2 and o2: Implication for resting-state functional con-

nectivity," *NeuroImage*, vol. 117, 2015, ISSN: 10959572. DOI: 10.1016/j.neuroimage.2015.05.035.

[19] B. Biswal, F. Z. Yetkin, V. M. Haughton, and J. S. Hyde, "Functional connectivity in the motor cortex of resting human brain using echo-planar mri," *Magnetic Resonance in Medicine*, vol. 34, 4 1995, ISSN: 15222594. DOI: 10.1002/mrm.1910340409.

[20] X. N. Zuo, A. D. Martino, C. Kelly, Z. E. Shehzad, D. G. Gee, D. F. Klein, F. X. Castellanos, B. B. Biswal, and M. P. Milham, "The oscillating brain: Complex and reliable," *NeuroImage*, vol. 49, 2 2010, ISSN: 10538119. DOI: 10.1016/j.neuroimage.2009.09.037.

[21] B. B. Biswal, M. Mennes, X. N. Zuo, S. Gohel, C. Kelly, S. M. Smith, C. F. Beckmann, J. S. Adelstein, R. L. Buckner, S. Colcombe, A. M. Dogonowski, M. Ernst, D. Fair, M. Hampson, M. J. Hoptman, J. S. Hyde, V. J. Kiviniemi, R. Kötter, S. J. Li, C. P. Lin, M. J. Lowe, C. Mackay, D. J. Madden, K. H. Madsen, D. S. Margulies, H. S. Mayberg, K. McMahon, C. S. Monk, S. H. Mostofsky, B. J. Nagel, J. J. Pekar, S. J. Peltier, S. E. Petersen, V. Riedl, S. A. Rombouts, B. Rypma, B. L. Schlaggar, S. Schmidt, R. D. Seidler, G. J. Siegle, C. Sorg, G. J. Teng, J. Veijola, A. Villringer, M. Walter, L. Wang, X. C. Weng, S. Whitfield-Gabrieli, P. Williamson, C. Windischberger, Y. F. Zang, H. Y. Zhang, F. X. Castellanos, and M. P. Milham, "Toward discovery science of human brain function," *Proceedings of the National Academy of Sciences of the United States of America*, vol. 107, 10 2010, ISSN: 00278424. DOI: 10.1073/pnas.0911855107.

[22] M. Borich, A. N. Babul, P. H. Yuan, L. Boyd, and N. Virji-Babul, "Alterations in resting-state brain networks in concussed adolescent athletes," *Journal of Neurotrauma*, vol. 32, 4 2015, ISSN: 15579042. DOI: 10.1089/neu.2013.3269.

[23] M. E. Raichle, A. M. MacLeod, A. Z. Snyder, W. J. Powers, D. A. Gusnard, and G. L. Shulman, "A default mode of brain function," *Proceedings of the National Academy of Sciences of the United States of America*, vol. 98, 2 2001, ISSN: 00278424. DOI: 10.1073/pnas.98.2.676.

[24] M. N. Moussa, M. R. Steen, P. J. Laurienti, and S. Hayasaka, "Consistency of network modules in resting-state fmri connectome data," *PLoS ONE*, vol. 7, 8 2012, ISSN: 19326203. DOI: 10.1371/journal.pone.0044428.

[25] F. X. Castellanos, A. D. Martino, R. C. Craddock, A. D. Mehta, and M. P. Milham, "Clinical applications of the functional connectome," *NeuroImage*, vol. 80, 2013, ISSN: 10538119. DOI: 10.1016/j.neuroimage.2013.04.083.

[26] J. L. Vincent, A. Z. Snyder, M. D. Fox, B. J. Shannon, J. R. Andrews, M. E. Raichle, and R. L. Buckner, "Coherent spontaneous activity identifies a hippocampal-parietal memory network," *Journal of Neurophysiology*, vol. 96, 6 2006, ISSN: 00223077. DOI: 10.1152/jn.00048.2006.

[27] B. T. T. Yeo, F. M. Krienen, J. Sepulcre, M. R. Sabuncu, D. Lashkari, M. Hollinshead, J. L. Roffman, J. W. Smoller, L. Zöllei, J. R. Polimeni, B. Fisch, H. Liu, and R. L. Buckner, "The organization of the human cerebral cortex estimated by intrinsic functional connectivity," *Journal of Neurophysiology*, vol. 106, 3 2011, ISSN: 00223077. DOI: 10.1152/jn.00338.2011.

[28] J. Thomas, D. Sharma, S. Mohanta, and N. Jain, "Resting-state functional networks of different topographic representations in the somatosensory cortex of macaque monkeys and humans," *NeuroImage*, vol. 228, 2021, ISSN: 10959572. DOI: 10.1016/j.neuroimage.2020.117694.

[29] K. Hwang, M. A. Bertolero, W. B. Liu, and M. D'Esposito, "The human thalamus is an integrative hub for functional brain networks," *Journal of Neuroscience*, vol. 37, 23 2017, ISSN: 15292401. DOI: 10.1523/JNEUROSCI.0067-17.2017.

[30] B. T. Yeo, F. M. Krienen, M. W. Chee, and R. L. Buckner, "Estimates of segregation and overlap of functional connectivity networks in the human cerebral cortex," *NeuroImage*, vol. 88, 2014, ISSN: 10538119. DOI: 10.1016/j.neuroimage.2013.10.046.

[31] R. W. Wang, W. L. Chang, S. W. Chuang, and I. N. Liu, "Posterior cingulate cortex can be a regulatory modulator of the default mode network in task-negative state," *Scientific Reports*, vol. 9, 1 2019, ISSN: 20452322. DOI: 10.1038/s41598-019-43885-1.

[32] W. Li, X. Mai, and C. Liu, "The default mode network and social understanding of others: What do brain connectivity studies tell us," *Frontiers in Human Neuroscience*, vol. 8, 1 FEB 2014, ISSN: 16625161. DOI: 10.3389/fnhum.2014.00074.

[33] Y. Xu, Q. Lin, Z. Han, Y. He, and Y. Bi, "Intrinsic functional network architecture of human semantic processing: Modules and hubs," *NeuroImage*, vol. 132, 2016, ISSN: 10959572. DOI: 10.1016/j.neuroimage.2016.03.004.

[34] S. Tanaka and E. Kirino, "Increased functional connectivity of the angular gyrus during imagined music performance," *Frontiers in Human Neuroscience*, vol. 13, 2019, ISSN: 16625161. DOI: 10.3389/fnhum.2019.00092.

[35] L. K. Ferreira and G. F. Busatto, "Resting-state functional connectivity in normal brain aging," *Neuroscience and Biobehavioral Reviews*, vol. 37, 3 2013, ISSN: 01497634. DOI: 10.1016/j.neubiorev.2013.01.017.

[36] J. S. Damoiseaux, C. F. Beckmann, E. J. Arigita, F. Barkhof, P. Scheltens, C. J. Stam, S. M. Smith, and S. A. Rombouts, "Reduced resting-state brain activity in the "default network" in normal aging," *Cerebral Cortex*, vol. 18, 8 2008, ISSN: 10473211. DOI: 10.1093/cercor/bhm207.

[37] H. Metwali and A. Samii, "Seed-based connectivity analysis of resting-state fmri in patients with brain tumors: A feasibility study," *World Neurosurgery*, vol. 128, 2019, ISSN: 18788769. DOI: 10.1016/j.wneu.2019.04.073.

[38] M. Göttlich, N. M. Jandl, J. F. Wojak, A. Sprenger, J. V. D. Gablentz, T. F. Münte, U. M. Krämer, and C. Helmchen, "Altered resting-state functional connectivity in patients with chronic bilateral vestibular failure," *NeuroImage: Clinical*, vol. 4, 2014, ISSN: 22131582. DOI: 10.1016/j.nicl.2014.03.003.

[39] A. Viard, J. Mutlu, S. Chanraud, F. Guenolé, P. J. Egler, P. Gérardin, J. M. Baleyte, J. Dayan, F. Eustache, and B. Guillery-Girard, "Altered default mode network connectivity in adolescents with post-traumatic stress disorder," *NeuroImage: Clinical*, vol. 22, 2019, ISSN: 22131582. DOI: 10.1016/j.nicl.2019.101731.

[40] D. S. Margulies, A. M. Kelly, L. Q. Uddin, B. B. Biswal, F. X. Castellanos, and M. P. Milham, "Mapping the functional connectivity of anterior cingulate cortex," *NeuroImage*, vol. 37, 2 2007, ISSN: 10538119. DOI: 10.1016/j.neuroimage.2007.05.019.

[41] D. M. Cole, S. M. Smith, and C. F. Beckmann, "Advances and pitfalls in the analysis and interpretation of resting-state fmri data," *Frontiers in Systems Neuroscience*, vol. 4, 2010, ISSN: 16625137. DOI: 10.3389/fnsys.2010.00008.

[42] C. F. Beckmann, M. DeLuca, J. T. Devlin, and S. M. Smith, "Investigations into resting-state connectivity using independent component analysis," *Philosophical Transactions of the Royal Society B: Biological Sciences*, vol. 360, 1457 2005, ISSN: 09628436. DOI: 10.1098/rstb.2005.1634.

[43] S. E. Joel, B. S. Caffo, P. C. V. Zijl, and J. J. Pekar, "On the relationship between seed-based and ica-based measures of functional connectivity," *Magnetic Resonance in Medicine*, vol. 66, 3 2011, ISSN: 15222594. DOI: 10.1002/mrm.22818.

[44] F. Z. Esfahlani, Y. Jo, J. Faskowitz, L. Byrge, D. P. Kennedy, O. Sporns, and R. F. Betzel, "High-amplitude cofluctuations in cortical activity drive functional connectivity," *Proceedings of the National Academy of Sciences of the United States of America*, vol. 117, 45 2020, ISSN: 10916490. DOI: 10.1073/pnas.2005531117.

[45] E. Bergmann, X. Gofman, A. Kavushansky, and I. Kahn, "Individual variability in functional connectivity architecture of the mouse brain," *Communications Biology*, vol. 3, 1 2020, ISSN: 23993642. DOI: 10.1038/s42003-020-01472-5.

[46] E. S. Finn, X. Shen, D. Scheinost, M. D. Rosenberg, J. Huang, M. M. Chun, X. Papademetris, and R. T. Constable, "Functional connectome fingerprinting: Identifying individuals using patterns of brain connectivity," *Nature Neuroscience*, vol. 18, 11 2015, ISSN: 15461726. DOI: 10.1038/nn.4135.

[47] C. Horien, X. Shen, D. Scheinost, and R. T. Constable, "The individual functional connectome is unique and stable over months to years," *NeuroImage*, vol. 189, 2019, ISSN: 10959572. DOI: 10.1016/j.neuroimage.2019.02.002.

[48] E. Amico and J. Goñi, "The quest for identifiability in human functional connectomes," *Scientific Reports*, vol. 8, 1 2018, ISSN: 20452322. DOI: 10.1038/s41598-018-25089-1.

[49] D. L. Murdaugh, T. Z. King, B. Sun, R. A. Jones, K. E. Ono, A. Reisner, and T. G. Burns, "Longitudinal changes in resting state connectivity and white matter integrity in adolescents with sports-related concussion," *Journal of the International Neuropsychological Society*, vol. 24, 8 2018, ISSN: 14697661. DOI: 10.1017/S1355617718000413.

[50] G. Murugesan, A. Famili, E. Davenport, B. Wagner, J. Urban, M. Kelley, D. Jones, C. Whitlow, J. Stitzel, J. Maldjian, and A. Montillo, "Changes in resting state mri networks from a single season of football distinguishes controls, low, and high head impact exposure," 2017. DOI: 10.1109/ISBI.2017.7950561.

[51] A. Powers, G. K. Murugesan, B. Saghafi, A. Montillo, J. Maldjian, E. Davenport, B. Wagner, D. Jones, J. Urban-Hobson, J. Stitzel, C. Whitlow, and M. Kelley, "Single season changes in resting state network power and the connectivity between regions distinguish head impact exposure level in high school and youth football players," 2018. DOI: 10.1117/12.2293199.

[52] B. Johnson, A. Dodd, A. R. Mayer, M. Hallett, and S. Slobounov, "Correction to: Are there any differential responses to concussive injury in civilian versus athletic populations: A neuroimaging study (brain imaging and behavior, (2020), 14, 1, (110-117), 10.1007/s11682-018-9982-1)," *Brain Imaging and Behavior*, vol. 14, 1 2020, ISSN: 19317565. DOI: 10.1007/s11682-018-0015-x.

[53] M. L. Alosco and R. A. Stern, "Youth exposure to repetitive head impacts from tackle football and long-term neurologic outcomes: A review of the literature, knowledge gaps and future directions, and societal and clinical implications," *Seminars in Pediatric Neurology*, vol. 30, 2019, ISSN: 15580776. DOI: 10.1016/j.spen.2019.03.016.

[54] E. McCuen, D. Svaldi, K. Breedlove, N. Kraz, B. Cummiskey, E. L. Breedlove, J. Traver, K. F. Desmond, R. E. Hannemann, E. Zanath, A. Guerra, L. Leverenz, T. M. Talavage, and E. A. Nauman, "Collegiate women's soccer players suffer greater cumulative head impacts than their high school counterparts," *Journal of Biomechanics*, vol. 48, 13 2015, ISSN: 18732380. DOI: 10.1016/j.jbiomech.2015.08.003.

[55] D. O. Svaldi, C. Joshi, E. C. McCuen, J. P. Music, R. Hannemann, L. J. Leverenz, E. A. Nauman, and T. M. Talavage, "Accumulation of high magnitude acceleration events predicts cerebrovascular reactivity changes in female high school soccer athletes," *Brain Imaging and Behavior*, vol. 14, 1 2020, ISSN: 19317565. DOI: 10.1007/s11682-018-9983-0.

[56] E. T. Campolettano, R. A. Gellner, E. P. Smith, S. Bellamkonda, C. T. Tierney, J. J. Crisco, D. A. Jones, M. E. Kelley, J. E. Urban, J. D. Stitzel, A. Genemaras, J. G. Beckwith, R. M. Greenwald, A. C. Maerlender, P. G. Brolinson, S. M. Duma, and S. Rowson, "Development of a concussion risk function for a youth population using head linear and rotational acceleration," *Annals of Biomedical Engineering*, vol. 48, 1 2020, ISSN: 15739686. DOI: 10.1007/s10439-019-02382-2.

[57] R. Beare, J. Chen, C. Adamson, T. Silk, D. Thompson, J. Yang, V. Anderson, M. Seal, and A. Wood, "Brain extraction using the watershed transform from markers.," *Frontiers in Neuroinformatics*, vol. 7, no. 32, Dec. 2013. DOI: doi:10.3389/fninf.2013.00032.

[58] X. Shen, F. Tokoglu, X. Papademetris, and R. T. Constable, "Groupwise whole-brain parcellation from resting-state fmri data for network node identification," *NeuroImage*, vol. 82, 2013, ISSN: 10538119. DOI: 10.1016/j.neuroimage.2013.05.081.

[59] L. Muresan, R. Renken, J. B. Roerdink, and H. Duifhuis, "Position-history and spin-history artifacts in fmri time series," vol. 4683, 2002. DOI: 10.1117/12.463613.

[60] P. E. Shrout and J. L. Fleiss, "Intraclass correlations: Uses in assessing rater reliability," *Psychological Bulletin*, vol. 86, 2 1979, ISSN: 00332909. DOI: 10.1037/0033-2909.86.2.420.

[61] S. S. Yoo, X. Wei, C. C. Dickey, C. R. Guttmann, and L. P. Panych, "Long-term reproducibility analysis of fmri using hand motor task," *International Journal of Neuroscience*, vol. 115, 1 2005, ISSN: 00207454. DOI: 10.1080/00207450490512650.

[62] B. B. Zandbelt, T. E. Gladwin, M. Raemaekers, M. van Buuren, S. F. Neggers, R. S. Kahn, N. F. Ramsey, and M. Vink, "Within-subject variation in bold-fmri signal changes across repeated measurements: Quantification and implications for sample size," *NeuroImage*, vol. 42, 1 2008, ISSN: 10538119. DOI: 10.1016/j.neuroimage.2008.04.183.

[63] K. O. McGraw and S. P. Wong, "Forming inferences about some intraclass correlation coefficients," *Psychological Methods*, vol. 1, 1 1996, ISSN: 1082989X. DOI: 10.1037/1082-989X.1.1.30.

[64] S. Kühn, C. G. Forlim, A. Lender, J. Wirtz, and J. Gallinat, "Brain functional connectivity differs when viewing pictures from natural and built environments using fmri resting state analysis," *Scientific Reports*, vol. 11, 1 2021, ISSN: 20452322. DOI: 10.1038/s41598-021-83246-5.

[65] M. Schurz, L. Maliske, and P. Kanske, "Cross-network interactions in social cognition: A review of findings on task related brain activation and connectivity," *Cortex*, vol. 130, 2020, ISSN: 19738102. DOI: 10.1016/j.cortex.2020.05.006.